Front. Phys. China, 2010, 5(2): 123–130
DOI 10.1007/s11467-010-0018-6

MINI-REVIEW ARTICLE

Molecule production via Feshbach resonance in bosonic systems

Jie LIU (刘杰)[1,2,†], **Bin LIU** (刘斌)[1]

[1] *Institute of Applied Physics and Computational Mathematics, P. O. Box 8009, Beijing 100088, China*
[2] *Center for Applied Physics and Technology, Peking University, Beijing 100084, China*
E-mail: liu_jie@iapcm.ac.cn

Received February 9, 2010; accepted March 14, 2010

In this article, we review our recent theoretical works on producing ultracold molecules from ultracold bosonic atoms via magnetically tunable Feshbach resonances. Our analysis relies on a two-channel quantum microscopic model that accounts for many-body effects in the association process. We show that the picture of two-body molecular production depicted by the Landau–Zener model is significantly altered due to many-body effects. We derive an analytic expression for molecular conversion efficiency for the nonadiabatic linearly swept Feshbach resonance, that explains the discrepancy between the prediction of the Landau–Zener formula and the experimental data. With including the thermal dephasing effects in the oscillating magnetic field modulation Feshbach resoance, we reproduce the Lorentzian resonance lineshape and explain the maximum conversion efficiency observed in experiment.

Keywords Feshbach resonance, molecule production, bosonic system

PACS numbers 03.75.Nt, 34.50.-s, 36.90.+f

Contents

1 Introduction

The conversion of ultracold atoms to ultracold molecules by time-varying magnetic fields in the vicinity of a Feshbach resonance is currently a topic of much experimental and theoretical interest. This particular conversion process lends itself well to the formation of molecular Bose-Einstein condensates (BECs) [1–4] and atom-molecule superpositions [5]. These Feshbach molecules and their creation process are also important for understanding ultracold fermionic systems in the BCS-BEC crossover regime because they are closely related to the pairing mechanism in a fermionic superfluid that occurs near a Feshbach resonance [6–9].

To date several techniques to produce Feshbach molecules have been demonstrated. A widely used technique involves the association of ultracold atoms into very weakly bound diatomic molecules by applying a linearly sweeping magnetic field across the Feshbach resonance. The underlying conversion dynamics are usually described by the Landau–Zener (LZ) model [10,11]. In Section 2, on the basis of the two-channel mean-field approach, we show that the many-body effects alter the LZ picture of two-body molecular production through dramatically distorting the energy levels near the Feshbach resonance, and derive an analytic expression for the conversion efficiency in the nonadiabatic regime. Our theory agrees with experimental data.

The linear sweeping technique inevitably heating the thermal clouds and limiting the atom-molecule conversion efficiency. Therefore an alternative efficient technique by applying a sinusoidally oscillating magnetic field modulation in the vicinity of a Feshbach resonance has been proposed [12]. In Section 3, review our work in this direction. We have investigated the mechanism un-

derlying the oscillating magnetic field modulation technique. By quantitatively including the thermal dephasing effect in the non-condensed atom clouds, our model has accounted for most experimental observations. Our model calculation has reproduced the Lorentzian resonance lineshape and explained the observed maximum conversion efficiency in terms of relaxation to a mean-field fixed point.

Finally, summary is presented in Section 4.

2 Feshbach resonance using linear sweeping magnetic field

2.1 Theoretical model

In this section, we focus on the Feshbach resonance using linearly sweeping magnetic field. Considering the experimental condition that the densities of the atom cloud is unusually low and the two- and three-body atomic decay and collisional molecular decay rates are negligible, we exploit the following two-channel model to describe the dynamics of converting atoms to molecules in the bosonic system,

$$\hat{H} = (\epsilon_a - \mu)\,\hat{a}^\dagger\hat{a} + [\epsilon_b + \nu(t) - 2\mu]\,\hat{b}^\dagger\hat{b} + \frac{g}{\sqrt{\mathcal{V}}}\left(\hat{a}^\dagger\hat{a}^\dagger\hat{b} + \hat{b}^\dagger\hat{a}\hat{a}\right) \quad (1)$$

Here, $\hat{a}$ ($\hat{a}^+$) and $\hat{b}(\hat{b}^+)$ are bose annihilation (creation) operators of atoms and molecules, respectively. The total number of particles $N = \hat{a}^\dagger\hat{a} + 2\hat{b}^\dagger\hat{b}$ is a conserved constant. The atomic and molecular kinetic energies are given by ϵ_a and ϵ_b, μ is the chemical potential, $\mathcal{V}$ denotes the quantization volume of trapped particles, therefore $n = N/\mathcal{V}$ is the mean density of initial bosonic atoms, $\nu(t)$ represents the magnetic detuning depends on the external field, $g = \sqrt{4\pi\hbar^2 a_{\rm bg}\Delta B\mu_{\rm co}/m}$ is the atom-molecule coupling due to the Feshbach resonance, m is the mass of a bosonic atom, $a_{\rm bg}$ is the background scattering length, ΔB is the width of the resonance, and $\mu_{\rm co}$ is the difference in the magnetic moment between the closed channel and open channel state. The external magnetic field is linearly swept from $B_{\rm in}$ to $B_{\rm end}$ with $B(t) = \dot{B}t$ and crosses the Feshbach resonance at B_0. When $|B_{\rm end} - B_{\rm in}| \gg \Delta B$, the magnetic detuning mainly contributed by the associated resonance energy $\nu(t) \simeq \mu_{\rm co}\,(B(t) - B_0)$ [13]. The total number of particles $N = \hat{a}^\dagger\hat{a} + 2\hat{b}^\dagger\hat{b}$ is a conserved constant.

Using the Fock states as a basis, the Schrödinger equation is written as:

$$\mathrm{i}\frac{\mathrm{d}}{\mathrm{d}t}|\psi\rangle = \hat{H}|\psi\rangle \quad (2)$$

where $|\psi\rangle = \sum_{j=0}^{N/2} c_j|2j, N/2-j\rangle, |2j, N/2-j\rangle = \frac{1}{\sqrt{(2j)!(N/2-j)!}}\left(\hat{a}^\dagger\hat{a}^\dagger\right)^j\left(\hat{b}^\dagger\right)^{N/2-j}|0\rangle$ $(j = 0, ..., N/2)$ are Fock states, and c_j is the probability amplitudes on the corresponding Fock state, respectively. The normalization condition is $\sum_j |c_j|^2 = 1$. By introducing $\epsilon = \nu(t) + \epsilon_b - 2\epsilon_a$ and $\eta = 2g\sqrt{n}$, the Schrödinger equation is rewritten as:

$$\mathrm{i}\frac{\mathrm{d}c_j}{\mathrm{d}t} = \sum_k H_{jk}c_k, \quad j, k = 0, 1, ..., N/2 \quad (3)$$

The Hamiltonian matrix elements are $H_{jk} = \langle 2j, N/2 - j|H|2k, N/2 - k\rangle$. For $j = k, H_{jj} = -\epsilon j$; for $j \neq k$, $H_{jk} = 0$ except $H_{j,j+1} = H_{j+1,j} = \eta\sqrt{(j+1)(2j+1)(N/2-j)/2N}$.

For the simplest case of $N = 2$, the above Eq. (3) reduce to the following two-level system of Landau–Zener type:

$$\mathrm{i}\hbar\frac{\mathrm{d}}{\mathrm{d}t}\begin{pmatrix} c_0 \\ c_1 \end{pmatrix} = \begin{pmatrix} 0 & \eta/2 \\ \eta/2 & -\epsilon \end{pmatrix}\begin{pmatrix} c_0 \\ c_1 \end{pmatrix} \quad (4)$$

where $|c_0|^2$ and $|c_1|^2$ denote the population of molecules and atoms, respectively. Initially, all particles populate in the lower level of the atomic state, i.e., $c_0 = 0, c_1 = 1$. When the external magnetic field is linearly swept across the Feshbach resonance at $B \simeq B_0$, a fraction of atoms will be converted to molecules at the avoided-crossing of energy levels. The conversion efficiency as a function of the sweeping rate (i.e., $\dot{\epsilon} = \mu_{\rm co}\dot{B}$) and coupling strength, takes the form [10, 11]:

$$\Gamma_{lz} = 1 - \exp\left(-\frac{\pi\eta^2}{2\hbar\dot{\epsilon}}\right) = 1 - \exp\left(-\frac{8\pi^2 n\hbar|a_{\rm bg}\Delta B|}{m|\dot{B}|}\right) \quad (5)$$

The above is the two-body molecular production picture and is consistent with the result from the coupled-channel scattering calculation in Ref. [14].

Mathematically, ignoring a total phase, the dynamics of Eq. (4) are equivalent to the following simple classical Hamiltonian [15, 16]:

$$\mathcal{H}_{lz} = \epsilon/\hbar s + \eta/\hbar\sqrt{1-s^2}\cos\theta \quad (6)$$

where the canonical conjugate variables are the population difference $s = |c_0|^2 - |c_1|^2$ and the relative phase $\theta = \arg c_0 - \arg c_1$. The dynamics are governed by the canonical equations of $\dot{\theta} = \frac{\partial\mathcal{H}_{lz}}{\partial s}, \dot{s} = -\frac{\partial\mathcal{H}_{lz}}{\partial\theta}$. The fixed points satisfying $\dot{s} = 0, \dot{\theta} = 0$ correspond to the extremum of system energy. These classical fixed points correspond to the eigenstates of quantum equations (4) and their energies (corresponding to the eigenvalues of quantum eigenstates) are calculated and plotted against the energy bias parameter ϵ in Fig. 1(a). It exhibits a typical LZ avoided-crossing configuration. Initially, all particles populate in the atomic state of $s_0 = -1$ at the left end of the lower level. When the external field passes through the Feshbach resonance of width $\eta/\hbar$ at

$B = B_0$, a fraction of atoms are converted to molecules at the right end of the lower level, leading to a variation in the population variable, i.e.,

$$s_f = 2\Gamma_{lz} - 1 = 1 - 2\exp\left(-\frac{\pi\eta^2}{2\hbar\dot{\epsilon}}\right) \tag{7}$$

As we go beyond the above two-body treatment to consider the many-body effects, the structure of the energy levels will change dramatically and the above LZ formula of the conversion efficiency will be altered due to many-body effects.

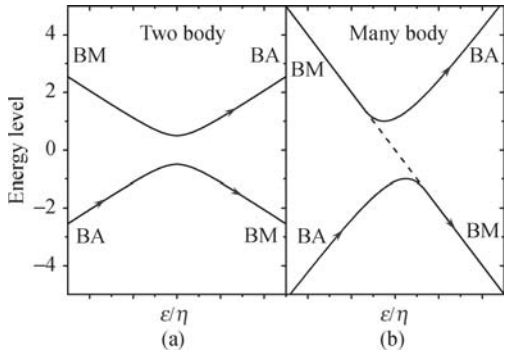

Fig. 1 Energy levels versus the scaled external magnetic fields. **(a)** Two-body Landau–Zener levels; **(b)** Many-body case ($N = \infty$), the dashed line represents an additional unstable eigenstate.

In order to include many-body effects, we introduce the operators to investigate the dynamics of this system [17],

$$\hat{K}_x = \sqrt{2}\frac{\hat{a}^\dagger\hat{a}^\dagger\hat{b} + \hat{b}^\dagger\hat{a}\hat{a}}{N^{3/2}} \tag{8}$$

$$\hat{K}_y = \sqrt{2}i\frac{\hat{a}^\dagger\hat{a}^\dagger\hat{b} - \hat{b}^\dagger\hat{a}\hat{a}}{N^{3/2}} \tag{9}$$

$$\hat{K}_z = \frac{2\hat{b}^\dagger\hat{b} - \hat{a}^\dagger\hat{a}}{N} \tag{10}$$

with the commutators

$$[\hat{K}_z, \hat{K}_x] = \frac{4\mathrm{i}}{N}\hat{K}_y \tag{11}$$

$$[\hat{K}_z, \hat{K}_y] = -\frac{4\mathrm{i}}{N}\hat{K}_x \tag{12}$$

$$[\hat{K}_x, \hat{K}_y] = \frac{\mathrm{i}}{N}\left(1 - \hat{K}_z\right)\left(1 + 3\hat{K}_z\right) + \frac{4\mathrm{i}}{N^2} \tag{13}$$

where $\hat{K}_x, \hat{K}_y$ denote the coherence terms, and $\hat{K}_z$ is the population imbalance. Then the Hamiltonian can be written as:

$$H = \frac{N}{4}\left(\epsilon\hat{K}_z + \sqrt{2}\eta\hat{K}_x\right) \tag{14}$$

Then the Heisenberg equations of motion are

$$\frac{\mathrm{d}}{\mathrm{d}t}\hat{K}_x = -\frac{1}{\hbar}\epsilon\hat{K}_y \tag{15}$$

$$\frac{\mathrm{d}}{\mathrm{d}t}\hat{K}_y = \frac{1}{\hbar}\epsilon\hat{K}_x - \frac{\eta}{\hbar}\frac{\sqrt{2}}{N} + \frac{\eta}{\hbar}\frac{3\sqrt{2}}{4}\left(\hat{K}_z - 1\right)\left(\hat{K}_z + \frac{1}{3}\right) \tag{16}$$

$$\frac{\mathrm{d}}{\mathrm{d}t}\hat{K}_z = \frac{\eta}{\hbar}\sqrt{2}\hat{K}_y \tag{17}$$

In the mean field limit where $N \to \infty$, all the commutators (11–13) vanish. Therefore, it is appropriate to replace K_x, K_y and K_z by their expected values u, v, and s, respectively. Then we have

$$\frac{\mathrm{d}}{\mathrm{d}t}u = -\frac{1}{\hbar}\epsilon v \tag{18}$$

$$\frac{\mathrm{d}}{\mathrm{d}t}v = \frac{1}{\hbar}\epsilon u + \frac{\eta}{\hbar}\frac{3\sqrt{2}}{4}(s-1)\left(s + \frac{1}{3}\right) \tag{19}$$

$$\frac{\mathrm{d}}{\mathrm{d}t}s = \frac{\eta}{\hbar}\sqrt{2}v \tag{20}$$

Noting the constraint $u^2 + v^2 = \frac{1}{2}(s-1)^2(s+1)$ and introducing the conjugate angular variable $\theta = \arctan(v/u)$ denoting the relative phase between atoms and molecules, the Heisenberg equations can be replaced by a classical Hamiltonian of the form:

$$\mathcal{H}_m = \epsilon/\hbar s + \eta/\hbar\sqrt{(1-s^2)(1-s)}\cos\theta \tag{21}$$

To understand the dynamics, we first look at the fixed points $\dot{s} = \dot{\theta} = 0$. The energies for these fixed points make up energy levels of the system, as shown in Fig. 1(b). The structure of these energy levels changes dramatically compared to the two-body case. We observe: (i) There are two fixed points when $|\epsilon/\eta|$ is large enough: one for the bosonic molecule (BM) and the other for the bosonic atom (BA). (ii) When $|\epsilon/\eta| < \sqrt{2}$, there is an additional fixed point with $s = 1$. However, this fixed point is a saddle point corresponding to dynamically unstable quantum states [18–20].

Compared to Hamiltonian (6), the coupling term in many-body Hamiltonian (21) is renormalized by a factor $\sqrt{1-s}$. So, the Fehsbach resonance width that is proportional to the coupling either broadens or shrinks depending on the factor. For the fast sweep case, s should be not far from its initial value -1, therefore, the resonance width broadens and we expect that many-body effects enhance the atom-molecule conversion. In contrast, for the slow sweep case, s may take a value close to 1, therefore, the resonance width shrinks. We then expect that the many-body effects suppress the atom–molecule conversion compared to the two-body Landau–Zener formula.

To derive an approximate analytic expression for the conversion efficiency, we introduce an effective coupling η_{eff} as:

$$\eta_{\mathrm{eff}} = \eta\sqrt{1-s^*} \tag{22}$$

where s^* can be approximately taken as the average between initial value $s_0 = -1$ and the final value s_f, i.e., $s^* = (-1 + s_f)/2$. Using the relation $\Gamma_m = 2\langle\hat{b}^\dagger\hat{b}\rangle/N = (1 + s_f)/2$ and formula (4), we obtain a self-consistent

formula for the many-body conversion efficiency Γ_m,

$$\Gamma_m \simeq 1 - \exp\left[-\frac{\pi\eta^2(2-\Gamma_m)}{2\hbar\dot{\epsilon}}\right] \tag{23}$$

The above self-consistent equation for the conversion efficiency Γ_m can be readily solved using the iteration method.

2.2 Comparison with experiment

Now we apply our theory to ^{85}Rb experiment by the JILA group [21]. Indeed, in the practical experiment the atoms are usually not condensed, the many modes are strongly coupled and the full Hamiltonian will read

$$\hat{H}^c = \sum_p (\epsilon_{a,p} - \mu)\,\hat{a}_p^\dagger \hat{a}_p + \sum_q [\epsilon_{b,q} + \nu(t) - 2\mu]\,\hat{b}_q^\dagger \hat{b}_q + \frac{g}{\sqrt{\mathcal{V}}} \sum_{p,q} \left(\hat{a}_{p+q/2}^\dagger \hat{a}_{-p+q/2}^\dagger \hat{b}_q + \hat{b}_q^\dagger \hat{a}_{-p+q/2} \hat{a}_{p+q/2}\right) \tag{24}$$

The kinetic energy distribution of the thermal particles are characterized by $k_{\rm B}T$, here $k_{\rm B}$ is the Boltzman constant, and T is the temperature. In the experiment, $k_{\rm B}T$ is much smaller than the effective Feshbach resonance width $g\sqrt{n}$, therefore we ignore the variation in the kinetic energy, i.e., $\epsilon_{a,p} \to \epsilon_a$ and $\epsilon_{b,q} \to \epsilon_b$. This approximation is tantamount to denote each "energy band" of the thermal particles by one energy level. In such approximation, the Hamiltonian (24) reduces to (1). Furthermore, we neglect the particle kinetic energy ϵ_a and ϵ_b. Then we have $\epsilon \simeq \mu_{\rm co}\,(B(t) - B_0)$.

In experiment, the atoms are held in a purely magnetic "baseball" trap. For efficient evaporation, the bias field is held at 162 G, where the scattering length is positive. For slow magnetic field ramps, Rb_2 molecules are produced only when the field is ramped upward through the resonance, which is located at 155 G. Hence, the first step in molecule production is to rapidly jump the magnetic field from 162 G to 147.5 G. They then sweep the field back up to 162 G at a chosen linear rate, producing molecules as they pass through the Feshbach resonance. The initial conditions of the atomic cloud are $N = 87\ 000$ and $n = 1.3 \times 10^{11}{\rm cm}^{-3}$. The Feshbach resonance parameters are $a_{\rm bg} = -443a_0, \Delta B = 10.71$ G, and $\mu_{\rm co} = -2.33\mu_{\rm B}$, where a_0 and $\mu_{\rm B}$ are the Bohr radius and Bohr magneton, respectively. The thermal cloud of the particles is at temperature $T = 40$ nK.

To compare with Landau–Zener theory quantitatively, the JILA group measured the ratio between mean density and $1/e$ ramp rate as a function of mean density. They found that the Landau–Zener parameter predicted from the two-body theory is roughly 1/8 of the value extracted from the experimental data. They use the formula $N_{\rm mol} = N_{\rm max}(1 - {\rm e}^{-\alpha n \Delta B a_{\rm bg}/\dot{B}})$ to fit the experimental data on molecular conversion, where $N_{\rm max}$ is the asymptotic number of molecules created for a very slow ramp, $\dot{B}$ is the magnetic field sweeping rate, α is a fitting parameter, and $\delta_{\rm LZ} = \alpha n \Delta B a_{\rm bg}/\dot{B}$ is the Landau–Zener parameter. The saturation data in Fig. 1(a) in Ref. [21] indicate that $N_{\rm max}/N = 37\%$. The $1/e$ ramp rate $\dot{B}_{1/e}$ is defined as that at $\dot{B}_{1/e}$, $\delta_{\rm LZ} = 1$ and $N_{\rm mol}/N_{\rm max} = 63\%$. It was then claimed that the data support a constant value for $n/\dot{B}_{1/e}$ (see Fig. 2). The value for α, extracted from the experimental data, is $4.5 \times 10^{-7}{\rm m}^2 \cdot {\rm s}^{-1}$. However, the two-body Landau-Zener formula (5) predicts $\alpha = 8\pi^2\hbar/m = 5.9 \times 10^{-8}{\rm m}^2 \cdot {\rm s}^{-1}$, roughly 1/8 of the experimental data.

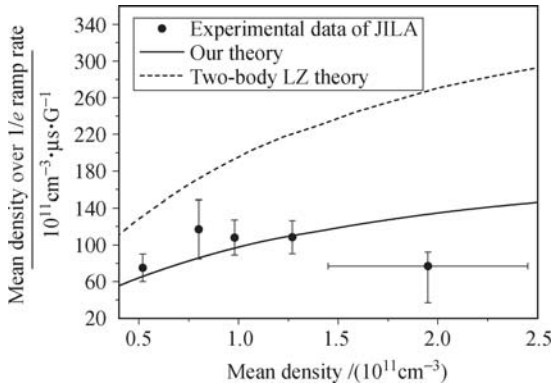

Fig. 2 The ratios of mean density over $1/e$ ramp rate, with respect to mean density. Our theory shows a good agreement with the experiment for four low density points but is obviously larger than the final point. At the high density, the cloud experienced significant heating during the ramps across the resonance, hence the density of the final point has significant uncertainty [21].

Now we apply our many-body theory to resolve this puzzle. At $B_{1/e}$, the molecular conversion efficiency is $N_{\rm mol}/N = 37\% \times 63\% = 23\%$. In the nonadiabatic regime, our many-body formula (23) is simplified as $\Gamma_m \simeq \dfrac{16\pi^2 n\hbar|a_{\rm bg}\Delta B|}{m|\dot{B}|}$. Substituting $\Gamma_m = 23\%, B = B_{1/e}$ into the above formula, we have $n/\dot{B}_{1/e} = \dfrac{0.23m}{16\pi^2\hbar|a_{\rm bg}\Delta B|} = 105 \times 10^{11}{\rm cm}^{-3}\cdot\mu{\rm s}\cdot{\rm G}^{-1}$, which is good agreement with the experimental data of the fourth scatter in Fig. 2.

To compare with two-body LZ formula Eq. (5), we see that, the many-body effects change the $1/e$ rate in the non-adiabatic regime by a factor of 2. The above analysis uncovers the physics behind the 1/8 deviation. The factor 1/8 is the product of following three factors: 0.37 is from the maximum conversion rate, 0.63 is from the definition of the $1/e$ ramp rate, and 1/2 comes from many-body effects.

Our calculations are extended to the cases of varied spatial densities. As mentioned above, in Ref. [21], the formula $N_{\rm mol} = N_{\rm max}(1 - {\rm e}^{-\alpha n \Delta B a_{\rm bg}/\dot{B}})$ is used to fit experimental data on molecular conversion. Accordingly, the $1/e$ ramp rate $B_{1/e}$ corresponds to $N_{\rm mol}/N_{\rm max} = 1 - 1/e = 63\%$. Our many-body theory Eq. (23) pre-

dicts that $n/\dot{B}_{1/e} = \dfrac{0.63m}{16\pi^2\hbar|a_{\rm bg}\Delta B|}\dfrac{N_{\rm max}}{N}$. Because the maximum molecular conversion efficiency (i.e., $N_{\rm max}/N$) is a function of peak phase space density as revealed in Fig. 2 in Ref. [21] and the spatial density is proportional to peak phase space density at the fixed temperature, we claim that $n/\dot{B}_{1/e}$ is spatial density n dependent through $N_{\rm max}/N$. The $N_{\rm max}/N$ as a function of density is read out from Fig. 2 in Ref. [21]. Thus, our theoretical curve is plotted against the experimental data in Fig. 2. It shows good agreement with the experiment for four low density points but is obviously larger than the final point. At high density, the cloud experienced significant heating during the ramps across the resonance, hence the density of the final point has significant uncertainty (i.e., see the caption of Fig. 1 of Ref. [21]). The result from two-body LZ theory is also presented in Fig. 2 for comparison. It is twice as large as that of many-body theory, and obviously deviates from the experimental data.

3 Feshbach resonance using oscillating magnetic field

3.1 Theoretical model

In this section we investigate the atom–molecule conversion using oscillating magnetic field modulation, in which around a fixed $B_{\rm ex}$ the magnetic field is modulated sinusoidally with small amplitude $B_{\rm mod}$ and the frequency ω, i.e.,

$$B(t) = B_{\rm ex} + B_{\rm mod}\sin(\omega t) \tag{25}$$

In order to increase the conversion efficiency, the $B_{\rm ex}$ is set to be in the vicinity of the Feshbach resonance, i.e., $|B_{\rm ex} - B_0| \ll \Delta B$. Under this condition, the magnetic detuning is mainly contributed by the binding energy, which expressed approximately as [12]:

$$\nu(t) \simeq -\frac{\hbar^2}{m(a_{\rm eff} - r_0)^2} \tag{26}$$

where r_0 is the effective range of the van der Waals potential, m is the mass of a bosonic atom, and $a_{\rm eff}$ denotes the effective scattering length driven by the external magnetic field:

$$a_{\rm eff} = a_{\rm bg}\left(1 - \frac{\Delta B}{B - B_0}\right) \tag{27}$$

Since $B_{\rm mod} \ll B_{\rm ex}$, the binding energy can be expanded into series to the first order of $B_{\rm mod}$:

$$\nu(t) = \nu_e + \nu_m\sin(\omega t) \tag{28}$$

where

$$\nu_e = -\frac{\hbar^2}{ma_{\rm bg}^2}\frac{(B_{\rm ex} - B_0)^2}{\left[\left(1 - \dfrac{r_0}{a_{\rm bg}}\right)(B_{\rm ex} - B_0) - \Delta B\right]^2} \tag{29}$$

and

$$\nu_m = \frac{\hbar^2}{ma_{\rm bg}^2}\frac{2(B_{\rm ex} - B_0)\Delta B B_{\rm mod}}{\left[\left(1 - \dfrac{r_0}{a_{\rm bg}}\right)(B_{\rm ex} - B_0) - \Delta B\right]^3} \tag{30}$$

Then we have $\epsilon = \nu_0 + \nu_m\sin(\omega t)$ with $\nu_0 = \nu_e + \epsilon_b - 2\epsilon_a$, and the mean-field Heisenberg equations (18)–(20) become

$$\frac{\rm d}{{\rm d}t}u = -\frac{1}{\hbar}\left[\nu_0 + \nu_m\sin(\omega t)\right]v \tag{31}$$

$$\frac{\rm d}{{\rm d}t}u = -\frac{1}{\hbar}\left[\nu_0 + \nu_m\sin(\omega t)\right]v + \frac{\eta}{\hbar}\frac{3\sqrt{2}}{4}(s-1)(s+\frac{1}{3}) \tag{32}$$

$$\frac{\rm d}{{\rm d}t}s = \frac{\eta}{\hbar}\sqrt{2}v \tag{33}$$

To get the time-averaged value of the conversion varied with different external field, we characterize each quantum trajectory by its time-averaged imbalance

$$-\langle\hat{K}_z\rangle_t \equiv -\frac{1}{\Delta t}\int_0^{\Delta t}{\rm d}t\langle\hat{K}_z\rangle(t) \tag{34}$$

employing the averaging interval $\Delta t \gg \hbar/\nu_0$. Figure 3 shows the results of such calculations by numerically solving the differential equations (3) for $N = 2, 20$ under periodic modulation with fixed scaled amplitude $\nu_m/\nu_0 = 0.2$ and frequencies ω ranging from 0 to $1.25\nu_0$. The solution of the mean-field equations (31)–(33) is also presented. There are several clear spikes that indicate the Shapiro-like resonance [22] in atom–molecule conversion driven by the external magnetic field.

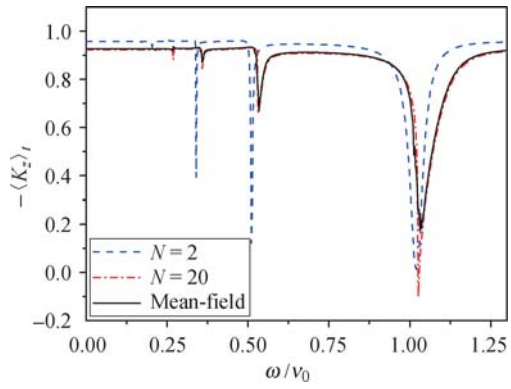

Fig. 3 Time-averaged population imbalance $-\langle\hat{K}_z\rangle_t$ for the driven system with different numbers of particles, tilt $\nu_0/\eta = 5$, and scaled driving amplitude $\nu_m = 1$.

These spikes indicate that the frequency of the modulated field is commensurate with the intrinsic frequencies of the atom–molecule conversion system in the absence of the periodic modulation. Now we analyze the intrinsic frequency. For $N = 2$, the commutators becomes

$$[\hat{K}_z, \hat{K}_x] = 2{\rm i}\hat{K}_y, \quad [\hat{K}_z, \hat{L}_y] = -2{\rm i}\hat{K}_x \tag{35}$$

$$[\hat{K}_x, \hat{K}_y] = {\rm i}\hat{K}_z \tag{36}$$

From the Heisenberg equations, we get

$$\frac{\mathrm{d}^2}{\mathrm{d}t^2}\hat{K}_y + \frac{1}{\hbar^2}\left(\nu_0^2+\eta^2\right)\hat{K}_y = 0 \tag{37}$$

Then the intrinsic frequency is readily obtained from the above equation as $\sqrt{\nu_0^2+\eta^2}/\hbar$. Thus, the center of resonance is expected to be $\sqrt{\nu_0^2+\eta^2}/(\hbar\omega) = p/q$ with p, q as integers. In our case, the resonances corresponding to $p/q = 1, 2, 3$ are more prominent. With N increasing, we find that the resonance center shifts to the right due to the many-body effect. We can obtain the intrinsic frequency in the mean-field limit, i.e., $N \to \infty$. From the mean-field Heisenberg equations (31–33), we readily obtain

$$\frac{\mathrm{d}^2}{\mathrm{d}t^2}v + \frac{1}{\hbar^2}\left(\nu_0^2+\eta^2(1-3s)\right)v = 0 \tag{38}$$

Initially all particles are in atom states, i.e., $s = -1$. Approximately substituting it into the above equation, we obtain the explicit expression of the frequency $\sqrt{\nu_0^2+4\eta^2}/\hbar$. This implies that, due to the many-body effect, the resonance centers shifts to $\sqrt{\nu_0^2+4\eta^2}/(\hbar\omega) = 1, 2, 3, ...$ The above theoretical analysis agrees with our numerical results.

3.2 Comparison with experiment

The generation of cold dimers from a cold Bose gas using an oscillating magnetic field has been implemented experimentally by the Wieman group at JILA [12]. It has shown that the method.

The thermal effect that is totally ignored in our previous discussions is important in the practical experiment. For a long time evolution, thermal particles scattering off the single-mode mean-field will cause phase diffusion at a rate proportional to the thermal cloud temperature, i.e., $\gamma = k_{\mathrm{B}}T/(2\pi\hbar)$ [23]. To account for the experimental data, we need to include the dephasing effect in our model. Modeling dephasing by fully including the quantum effects requires sophisticated theoretical studies. The standard approaches of quantum optics for open systems involve quantum kinetic master equations. Here, we adopt the simple mean-field treatment in our model. From the mean-field viewpoint, the decoherence term introduces a γ transversal relaxation term into the mean-field Heisenberg equations of motion according to [18–20, 24]

$$\frac{\mathrm{d}}{\mathrm{d}t}u = -\frac{1}{\hbar}\epsilon v - \gamma u \tag{39}$$

$$\frac{\mathrm{d}}{\mathrm{d}t}v = \frac{1}{\hbar}\epsilon u + \frac{\eta}{\hbar}\frac{3}{4}\sqrt{2}\,(s-1)\left(s+\frac{1}{3}\right) - \gamma v \tag{40}$$

$$\frac{\mathrm{d}}{\mathrm{d}t}s = \frac{\eta}{\hbar}\sqrt{2}v \tag{41}$$

The imbalance of atom-pairs and molecules s is varied in the range of $[-1, 1]$ with the lower limit corresponding to a pure atomic gas and $s = 1$ for a pure molecular gas. What we are concerned about is, after the conversion process, how many atomic pairs are converted to molecules.

Now we apply our theory to the experiment of ^{85}Rb in Ref. [12]. The atoms are held in a purely magnetic trap at a bias field of B_r. After evaporative cooling, the magnetic field B is linearly swept to a selected value at B_{ex}, and then a sinusoidal magnetic field pulse with peak-to-peak amplitude B_{mod} and modulation frequency ω for a duration of the coupling time is applied. The swept magnetic field can be expressed as:

$$B = \begin{cases} B_r - \alpha_r t, & 0 \leqslant t < t_0 \\ B_{\mathrm{ex}} + B_{\mathrm{mod}}\sin(\omega t), & t_0 \leqslant t < t_0 + t_{\mathrm{c}} \\ B_{\mathrm{ex}} + \alpha_r t, & t_0 + t_{\mathrm{c}} \leqslant t < 2t_0 + t_{\mathrm{c}} \end{cases} \tag{42}$$

where $B_r = 162$ G, $B_{\mathrm{ex}} = 156.5$ G, $B_{\mathrm{mod}} = 0.13$ G, ω ranges from 2 kHz to 9 kHz, t_0 is the linear sweep time, $\alpha_r = (B_r - B_{\mathrm{ex}})/t_0$ is the linear sweep rate, and t_{c} is the coupling time. For the thermal cloud, with temperature T, one molecule has 5 degrees of freedom while two atoms have 6 degrees of freedom; according to the equipartition theorem, we have $(2\epsilon_a - \epsilon_b) \approx k_{\mathrm{B}}T/2$. The scaled parameters in Eq. (39)–(41) are

$$\nu(t) = -\frac{\hbar^2}{m a_{\mathrm{bg}}^2}\frac{(B-B_0)^2}{\left[\left(1-\dfrac{r_0}{a_{\mathrm{bg}}}\right)(B-B_0) - \Delta B\right]^2} \tag{43}$$

and

$$\eta = 2\sqrt{4\pi\hbar^2|a_{\mathrm{bg}}\mu_{\mathrm{co}}|\Delta B n/m} \tag{44}$$

The experimental parameters are $r_0 = 185a_0$ [25, 26], $B_0 = 155$ G, the temperature $T = 20$ nK, and density $n = 10^{11}\mathrm{cm}^{-3}$. At this location B_{ex}, the difference of magnetic moment is $\mu_{\mathrm{co}} = \partial\nu(t)/\partial B = 1.2\times10^{-4}\mu_{\mathrm{B}}$, which is extracted from the experimental data [27]. Figure 4 shows the conversion efficiency as a function of modulation frequency for three different coupling times. The resonance line width is broadened by the dephasing term. There is a clear Lorentzian distribution resonance at frequency about 6.25 kHz, close to the experiment. Except the fundamental frequency resonance at $\omega = 6.25$ kHz, there is also a weakly $(2:1)$ mode resonance at about $\omega = 3.1$ kHz, which has not been observed in an experiment. Our linewidth is approximately 0.3 kHz at the zero conversion limit, as shown in the subfigure. In the experiment, it is about 0.2 kHz.

In Fig. 5, we show the conversion efficiency with respect to coupling time. The squares with error bars are experimental data in Ref. [12]. For temperature $T = 20$ nK and density $n = 10^{11}\mathrm{cm}^{-3}$, our results are close to the experimental data. We also show the cases of different temperatures by considering the isobaric condition, i.e., $nT = const$. The above calculation shows

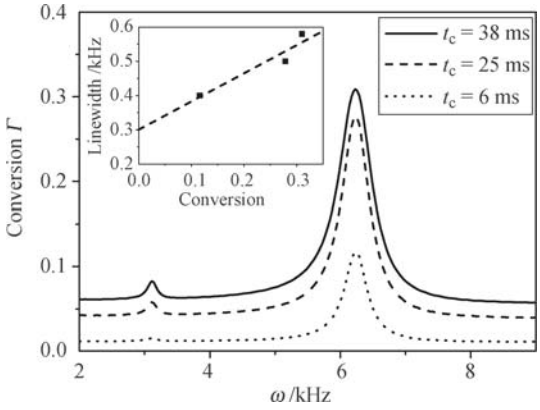

Fig. 4 Conversion efficiency of atoms converted to molecules as a function of modulation frequency for three different coupling times. For a fixed coupling time, the curve can be fitted by a Lorentzian distribution $\Gamma = \Gamma_0 + \frac{2A}{\pi}\frac{\Delta}{4(\omega-\omega_c)^2+\Delta^2}$, e.g., for $t_c = 38$ ms, the fitting parameters are $\Gamma_0 = 0.06$, $\omega_c = 6.2, \Delta = 0.6, A = 0.23$. In the subfigure, by fitting the linewidth versus conversion data to a straight line, we find the zero conversion limit to be 0.3 kHz.

that increasing the temperature will lessen the molecular production because the dephasing term is proportional to the temperature. On the other aspesct, the conversion efficiency decreases with the increasing of temperature. For different temperatures, a common feature is that the conversion efficiency increases with the coupling time until the conversion efficiency becomes saturated at 1/3. This can be explained from investigating Eq. (39)–(41), where $u = v = 0, w = -1/3$ is the fixed point in the absence of the dephasing term. The observed limit in atom–molecule conversion efficiency has been extensively discussed, including the Landau–Zener (LZ) model of two-body molecular production [14], phase-space density model [21], equilibration model at finite temperatures [28]. Our above investigation suggests a new mechanism for the observed maximum efficiency: The system is found to relax into the mean-field fixed point due to the dephasing effect.

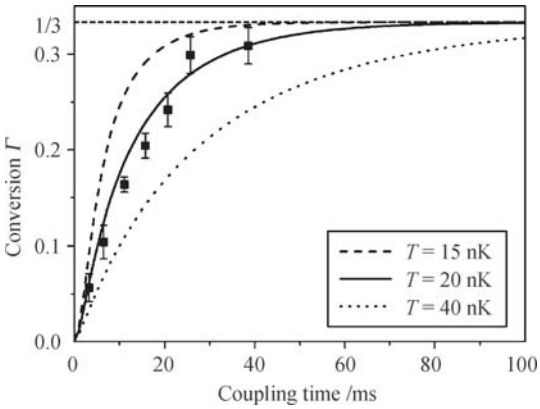

Fig. 5 Conversion efficiency of atoms converted to molecules under a periodic modulation with amplitude $B_{\rm mod} = 0.13$ G and frequency $\omega = 6.25$ kHz with respect to coupling time for different temperatures. The squares with error bars are from Fig. 4(a) of Ref. [12]. The conversion of ultracold atoms to molecules increases with the coupling time until it becomes saturated at 1/3.

4 Conclusion

In summary, we have thoroughly investigated the dynamics of ultracold molecule production from ultracold bosonic atom gas via magnetically tunable Feshbach resonance on the basis of a two-channel quantum microscopic model. With the mean-field approach, we have analysed the model theoretically and accounted for the experiment for the linearly sweeping Feshbach resoance as well as for the oscillating modulation Feshbach resonance. It is shown that the picture of two-body molecular production depicted by the Landau–Zener model is significantly altered due to many-body effects. In this paper, our review is confined to our works on the bosonic systems [32, 33]. For the fermionic systems, we also make thoroughly investigation, details refer to Ref. [34].

Acknowledgements We thank Prof. Gang Hu for his Kind invitation of writting this review.

References

1. M. Greiner, C. A. Regal, and D. S. Jin, Nature (London), 2003, 426: 537
2. M. W. Zwierlein, C. A. Stan, C. H. Schunck, S. M. F. Raupach, S. Gupta, Z. Hadzibabic, and W. Ketterle, Phys. Rev. Lett., 2003, 91: 250401
3. S. Jochim, M. Bartenstein, A. Altmeyer, G. Hendl, S. Riedl, C. Chin, J. Hecker Denschlag, and R. Grimm, Science, 2003, 302: 2101
4. M. Bartenstein, A. Altmeyer, S. Riedl, S. Jochim, C. Chin, J. Hecker Denschlag, and R. Grimm, Phys. Rev. Lett., 2004, 92: 120401
5. E. A. Donley, N. R. Claussen, S. T. Thompson, and C. E. Wieman, Nature (London), 2002, 417: 529
6. M. Holland, S. J. J. M. F. Kokkelmans, M. L. Chiofalo, and R. Walser, Phys. Rev. Lett., 2001, 87: 120406
7. E. Timmermans, K. Furuya, P. W. Milloni, and A. K. Kerman, Phys. Lett. A, 2001, 285: 228
8. M. W. Zwierlein, C. A. Stan, C. H. Schunck, S. M. F. Raupach, A. J. Kerman, and W. Ketterle, Phys. Rev. Lett., 2004, 92: 120403
9. M. Greiner, C. A. Regal, and D. S. Jin, Phys. Rev. Lett., 2005, 94: 070403
10. L. D. Landau, Phys. Z. Sowjetunion, 1932, 2: 46
11. G. Zener, Proc. R. Soc. London, Ser. A, 1932, 137: 696
12. S. T. Thompson, E. Hodby, and C. E. Wieman, Phys. Rev. Lett., 2005, 95: 190404
13. T. Köhler and K. Góral, Rev. Mod. Phys., 2006, 78: 1311
14. K. Góral, T. Köhler, S. A. Gardiner, E. Tiesinga, and P. S. Julienne, J. Phys. B, 2004, 37: 3457
15. J. Liu, L. B. Fu, B. Y. Ou, S. G. Chen, D. I. Choi, B. Wu, and Q. Niu, Phys. Rev. A, 2002, 66: 023404

16. J. Liu, B. Wu, and Q. Niu, Phys. Rev. Lett., 2003, 90: 170404
17. A. Vardi, V. A. Yurovsky, and J. R. Anglin, Phys. Rev. A, 2001, 64: 063611
18. J. R. Anglin, Phys. Rev. A, 2003, 67: 051601
19. J. Liu, C. W. Zhang, M. G. Raizen, and Q. Niu, Phys. Rev. A, 2006, 73: 013601
20. G. F. Wang, D. F. Ye, L. B. Fu, X. Z. Chen, and J. Liu, Phys. Rev. A, 2006, 74: 033414
21. E. Hodby, S. T. Thompson, C. A. Regal, M. Greiner, A. C. Wilson, D. S. Jin, E. A. Cornell, and C. E. Wieman, Phys. Rev. Lett., 2005, 94: 120402
22. S. Shapiro, Phys. Rev. Lett., 1963, 11: 80
23. See, for example, E. Eisenberg, K. Held, and B. L. Altshuler, Phys. Rev. Lett., 2002, 88: 136801
24. J. R. Anglin and A. Vardi, Phys. Rev. A, 2001, 64: 013605
25. R. A. Duine and H. T. C. Stoof, New J. Phys., 2003, 5: 69
26. G. F. Gribakin and V. V. Flambaum, Phys. Rev. A, 1993, 48: 546
27. N. R. Claussen, S. J. J. M. F. Kokkelmans, S. T. Thompson, E. A. Donley, E. Hodby, and C. E. Wieman, Phys. Rev. A, 2003, 67: 060701(R)
28. J. E. Williams, N. Nygaard, and C. W. Clark, New J. Phys., 2006, 8: 150
29. A. Sinatra and Y. Castin, Phys. Rev. A, 2008, 78: 053615
30. A. Sinatra, Y. Castin, and E. Witkowska, Phys. Rev. A, 2009, 80: 033614
31. A. A. Norrie, R. J. Ballagh, and C. W. Gardiner, Phys. Rev. A, 2006, 73: 043617
32. J. Liu, B. Liu, and L. B. Fu, Phys. Rev. A, 2008, 78: 013618
33. B. Liu, L. B. Fu, and J. Liu, Phys. Rev. A, 2010, 81: 013602
34. J. Liu, L. B. Fu, B. Liu, and B. Wu, New J. Phys., 2008, 10: 123018